

Effects of post-calcination and mechanical pulverization on the electrochemical properties of nano-sized $\text{Li}_4\text{Ti}_5\text{O}_{12}$ for hybrid capacitors



Byung-Gwan Lee ^{a, b}, Hyo-Jin Ahn ^{b, **}, Jung-Rag Yoon ^{a, *}

^a R&D Center, Samwha Capacitor Co., Ltd, Youngin 17118, Republic of Korea

^b Program of Materials Science & Engineering, Convergence Institute of Biomedical Engineering and Biomaterials, Seoul National University of Science and Technology, Seoul 01811, Republic of Korea

ARTICLE INFO

Article history:

Received 31 July 2016

Received in revised form

3 October 2016

Accepted 26 October 2016

Available online 27 October 2016

Keywords:

$\text{Li}_4\text{Ti}_5\text{O}_{12}$

Lithium titanate

Post-calcination

Mechanical pulverization

ABSTRACT

Great efforts have been devoted for the synthesis of $\text{Li}_4\text{Ti}_5\text{O}_{12}$ nanoparticles as anode material, because particle size less than 100 nm is the main factor for achieving a high rate capability. In this study, we fabricated nano-sized $\text{Li}_4\text{Ti}_5\text{O}_{12}$ by high-energy milling operated at 3500 rpm, that it was treated afterwards by post-calcination to improve its pulverized crystallinity. Post-calcination at moderate temperature is found to be effective for improving the electrochemical properties of $\text{Li}_4\text{Ti}_5\text{O}_{12}$ prepared by mechanical pulverization. Finally, a 100 nm-sized $\text{Li}_4\text{Ti}_5\text{O}_{12}$ was successfully obtained by optimizing the high-energy milling passing 10 times in chamber and setting post-calcination to 700 °C. The specific capacity significantly depended on the crystallinity of $\text{Li}_4\text{Ti}_5\text{O}_{12}$ after treated by the post-calcination. The 100 nm-sized $\text{Li}_4\text{Ti}_5\text{O}_{12}$ showed high-rate capability and good capacity retention of 99.9% after 1500 cycles. It can be explained by the synergistic effect of reduced particle size and improved crystallinity.

© 2016 Published by Elsevier B.V.

1. Introduction

Nowadays, owing to the worldwide growth, high-efficiency and low-manufacturing cost has become a major challenge for nano-sized particle fabrication. In particular, there is primarily high demand for nano-sized materials that can lead to a high-rate capability of lithium ion. The spinel $\text{Li}_4\text{Ti}_5\text{O}_{12}$ has attracted much attention as one of the most promising anode materials for hybrid capacitors and lithium ion batteries. The reason is because it has good structural stability with nearly zero strain upon the intercalation/deintercalation of Li^+ , a flat operating potential at about 1.55 V vs. Li^+/Li with a theoretical capacity of 175 mAhg^{-1} , and an excellent cycling performance [1–7]. Despite of its advantages, the low electrical conductivity (10^{-9} S/cm) and its Li-ion diffusion coefficient results in poor rate capability [8–10]. To overcome these shortcomings, many studies relative to the reducing diffusion path for high-rate capability, such as the synthesis of nanocrystalline

particles [3,11], improving the electrical conductivity by surface modification [2] and transition metal ion doping [12], have been conducted. In particular, the design of nanocrystalline particles is applicable to active materials that exhibit low electrical conductivity like $\text{Li}_4\text{Ti}_5\text{O}_{12}$, because it leads to a shorter transport distance of Li ions, and increase the contact area between electrode and electrolyte for high power.

$\text{Li}_4\text{Ti}_5\text{O}_{12}$ has been mostly synthesized by solid-state reaction of stoichiometric samples of TiO_2 and Li_2CO_3 . In spite of its convenience for larges scale fabrications, the solid state reaction process usually can not synthesize $\text{Li}_4\text{Ti}_5\text{O}_{12}$ with particle size less than 300 nm, because the reaction between TiO_2 and Li_2CO_3 takes place at high temperatures over 800 °C. As a result, it may strongly affect their high-rate performance during the charging and discharging processes. Nowadays, modern high-energy mills facilitate pulverization of powder with nanometer particle size by mechanical force. Therefore, high-energy mechanical milling achieves applications that produces materials with metastable and nanocrystalline phases. $\text{Li}_4\text{Ti}_5\text{O}_{12}$ is one such material wherein there exists a need to fabricate nanoscale particles in order to render it suitable for high-rate capability.

In this study, nano-sized particles were successfully prepared by a solid-state reaction with the help of high-energy milling using

* Corresponding author.

** Corresponding author.

E-mail addresses: hjahn@seoultech.ac.kr (H.-J. Ahn), yojungrag@samwha.com (J.-R. Yoon).

fine ZrO₂ beads [12]. We propose the following three-step process: (1) synthesis of sub-micron sized Li₄Ti₅O₁₂ by solid-state reaction, (2) pulverization by high energy milling, and (3) crystallinity improvement by post-calcination. Li₄Ti₅O₁₂ with a particle size of 1 μm was prepared by a conventional solid-state reaction at 900 °C. There were ten attempts to pulverize sub-micron sized Li₄Ti₅O₁₂ by high energy mechanical milling. Then, to improve the crystallinity of the Li₄Ti₅O₁₂ weakened by pulverization, post-calcination was carried out at 500, 600, and 700 °C, respectively. Finally, nano-sized Li₄Ti₅O₁₂ powders with excellent rate capability were successfully obtained. Their electrochemical performance were also investigated by hybrid capacitors.

2. Experiment details

2.1. Synthesis and characterization of Li₄Ti₅O₁₂ powder

TiO₂ (99.9%) and Li₂CO₃ (99.6%) as starting materials were purchased from SHOWA DENKO(JAPAN) and Japan Pulp and Paper, respectively. Stoichiometric samples of Ti and Li, at a 5:4 rate, were mixed in ethanol (99.9%). Micron-sized Li₄Ti₅O₁₂ was synthesized from TiO₂ and Li₂CO₃ by solid-state reaction at 900 °C. In order to fabricate nano-sized Li₄Ti₅O₁₂, ten batches of the Li₄Ti₅O₁₂ in ethanol solvent were pulverized by high-energy milling (NS-002, DINTEK, KOREA) operated at 3500 rpm using 0.1 mm ZrO₂ beads. All ten batches were passed into the chamber of milling machine 1, 4, 7, and 10 times pass for 5 min. Then post-calcination with Li₄Ti₅O₁₂ powders passed 10 times in chamber were carried out at 500, 600, and 700 °C for 2 h, respectively. The X-ray diffractions of the samples were recorded with Cu K_α (λ = 1.5406 Å) radiation using a diffraction angle of 2θ ranging from 10 to 80° at a scan rate of 5° min⁻¹. The particle size distribution was identified by laser particle size analyzer (HORIBA LA-900). Specific surface areas were evaluated by N₂ gas adsorption and desorption measurements (TriStar) using the Brunauer–Emmett–Teller (BET) method. The morphologies of the samples were characterized by field emission scanning electron microscopy (FE-SEM, JEOL JSM-7500F).

2.2. Preparation of hybrid capacitor and electrochemical measurements

For negative electrodes, Li₄Ti₅O₁₂ powders were mixed with conductive carbon black (Super-P Li) and polyvinylidene fluoride (PVDF) in the weight ratio 80:10:10 in *N*-methyl pyrrolidinone (NMP) solvent. The negative electrodes are pressed to obtain a desired thickness (thickness = 60 μm, electrode density of 1.17 g cm⁻³). The positive electrodes were prepared by mixing activated carbon, conductive carbon black, and polytetrafluoroethylene (PTFE) in the weight ratio 75:15:10 in de-ionized water. The positive electrodes with the electrode density of 0.53 g cm⁻³ are pressed as negative electrodes. For preparation of hybrid capacitors, negative and positive electrode ratio was 0.25. The electrochemical properties of the Li₄Ti₅O₁₂ synthesized by different post-calcination temperatures were examined using hybrid capacitors combined with an activated carbon positive electrode. In dry room (dew point -75 °C), positive electrode, separator, and negative electrode were assembled. Before being impregnated in an electrolyte solution of 1.0 M LiPF₆/acetonitrile, the cells were dried in a vacuum oven for 48 h to remove moisture. Finally, the hybrid capacitors were assembled as a cylindrical cell (Φ22 × 45 mm). The electrochemical performance was evaluated in the potential range from 1.5 to 2.8 V at various current densities of 1, 5, 10, 15, and 20 A using a programmable multichannel battery tester (Arbin Instruments). The impedance measurements were carried out using IviumSoft impedance analyzer in the frequency range from 0.1 to 100 kHz.

3. Results and discussion

Fig. 1 shows the particle size distribution (PSD) of the Li₄Ti₅O₁₂ prepared by a high-energy mechanical milling. PSD analysis can confirm the diameter of Li₄Ti₅O₁₂ aggregate. Their stability, even after ultra-sonication, indicates fusion of the primary crystals [13]. As Li₄Ti₅O₁₂ powders are repeatedly passed into milling machine 1, 4, 7, and 10 times pass, average particle size of Li₄Ti₅O₁₂ aggregate tends to decrease by high energy milling. The average particle size no longer decreases after 10 times pass. It is clear that Li₄Ti₅O₁₂ after 10 pass exhibits a more narrow size distribution in comparison with the pristine one. The average particle size of pristine Li₄Ti₅O₁₂ aggregate is 77.6 μm (D₅₀) and that of Li₄Ti₅O aggregate after 10 times pass is 0.17 μm (D₅₀). The particle size distribution and BET of Li₄Ti₅O₁₂ after 10 times pass and pristine Li₄Ti₅O₁₂ are listed in Table 1.

Fig. 2 shows SEM images of the Li₄Ti₅O₁₂ particles pulverized by high energy milling. The primary particle size decreases with an increase in the number of pulverization. This trend in Li₄Ti₅O₁₂ size change is consistent with the milling number by high-energy milling. The primary particle size of the Li₄Ti₅O₁₂ prepared by 10 times pass in the milling chamber is less than 50 nm.

Fig. 3 shows the XRD patterns of pristine and pulverized Li₄Ti₅O₁₂ powders. The XRD pattern of the pristine one was well formed as previously reported [14]. In the initial stage of pulverization, the XRD patterns of Li₄Ti₅O₁₂ (1 time pass) show similar shapes to the pristine one without any secondary phases. However, diffraction peaks show a tendency to decrease in intensity and broaden with an increase in the number of pulverization. It could be explained in terms of the microstructural refinement and micro-strain generated by the intense plastic deformation developed in the Li₄Ti₅O₁₂ during high-energy milling. When mechanical milling is used for pulverization, the powder particles either remain unchanged or are fractured into smaller particles in the milling process. In case of high-energy mechanical milling, plastic deformation could take place along powder particles, because of dramatic and structural changes during milling [15]. In order to improve the crystallinity of pulverized Li₄Ti₅O₁₂, post-calcination with Li₄Ti₅O₁₂ powders passed 10 times in the milling chamber was carried out at 500 (denoted as LTO500), 600 (denoted as LTO600), and 700 °C (denoted as LTO700), respectively. Fig. 4 shows the X-ray peaks of the Li₄Ti₅O₁₂ treated by post-calcination after pulverization (10

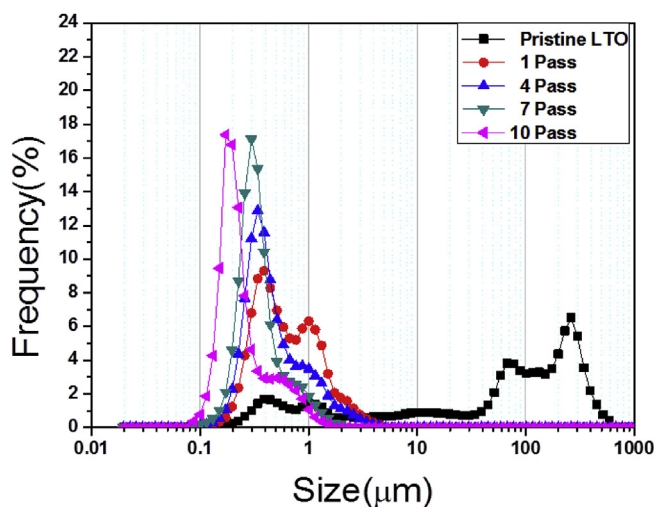
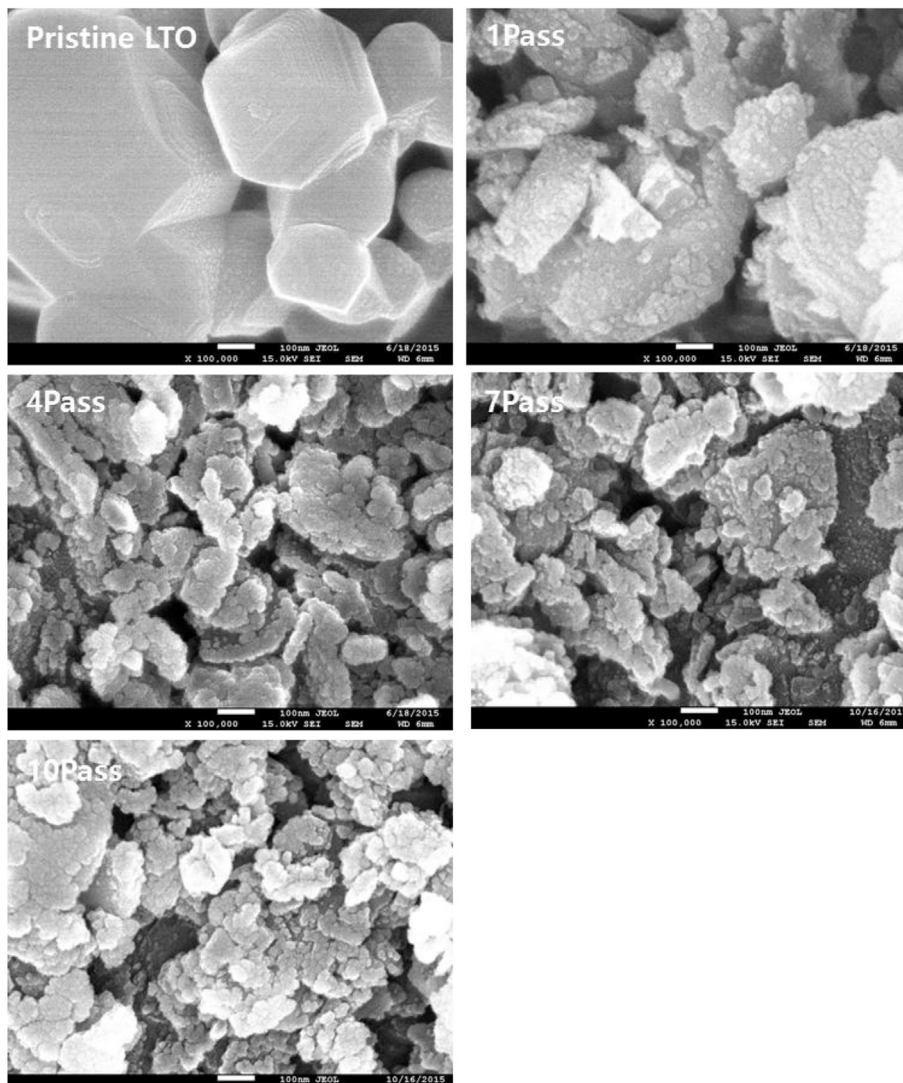


Fig. 1. Particle size distribution of pristine Li₄Ti₅O₁₂ and Li₄Ti₅O₁₂ powders obtained by high-energy milling 1, 4, 7, and 10 times pass.

Table 1The particle size distribution and BET of $\text{Li}_4\text{Ti}_5\text{O}_{12}$ after 10 times pass and pristine $\text{Li}_4\text{Ti}_5\text{O}_{12}$.

Materials	D10 (μm)	D50 (μm)	D90 (μm)	BET ($\text{m}^2 \text{g}^{-1}$)
$\text{Li}_4\text{Ti}_5\text{O}_{12}$ after 10 times pass	0.05	0.17	0.87	24.4
Pristine $\text{Li}_4\text{Ti}_5\text{O}_{12}$ (no pulverization)	0.59	77.63	287.70	3.2

**Fig. 2.** SEM images of pristine $\text{Li}_4\text{Ti}_5\text{O}_{12}$ and $\text{Li}_4\text{Ti}_5\text{O}_{12}$ powders obtained by high-energy milling 1, 4, 7, and 10 times pass.

times pass). The peak intensities of the $\text{Li}_4\text{Ti}_5\text{O}_{12}$ clearly increase with increasing post-calcination temperature, suggesting a crystallinity improvement of pulverized $\text{Li}_4\text{Ti}_5\text{O}_{12}$. With increased post-calcination temperature, the primary particle size also was increased as shown in Fig. 5. In case of LTO500 with particle size less than 50 nm, there is almost no change in particle size in comparison with the 10 times pass $\text{Li}_4\text{Ti}_5\text{O}_{12}$ (no post-calcination). On the other hand, for LTO700, submicron-sized $\text{Li}_4\text{Ti}_5\text{O}_{12}$ are assembled with about 100 nm primary nanoparticles. It is obvious that the grain size of $\text{Li}_4\text{Ti}_5\text{O}_{12}$ primary particles increase with increasing post-calcination temperatures from 500 to 700 °C, indicating a grain growth of $\text{Li}_4\text{Ti}_5\text{O}_{12}$ primary particles. However, its particle size is still very small compared to pristine LTO, as shown in Fig. 2.

In order to evaluate $\text{Li}_4\text{Ti}_5\text{O}_{12}$ powders obtained by post-

calcinations at 500, 600, and 700 °C, hybrid capacitors were fabricated in combination with activated carbon electrodes. The charge/discharge curves of the hybrid capacitors using LTO500, LTO600, LTO700, and pristine LTO were measured at 1 A as shown in Fig. 6, exhibiting a similar shape. At the beginning of the discharge, a dramatically falling region was observed for about 0.2 s. This is known as the uncompensated resistance and is caused by the internal resistance of electrode materials, especially $\text{Li}_4\text{Ti}_5\text{O}_{12}$ due to its slow Li-ion kinetics [16,17]. Synthesis of nano-sized $\text{Li}_4\text{Ti}_5\text{O}_{12}$ with high purity, controllable crystallinity, and uniform sizes is an important factor for high power density. LTO700 exhibits a pure LTO phase with improved crystallinity compared with LTO500, despite its bigger particle size. The calculated specific capacitances of LTO500, LTO600, LTO700, and pristine LTO are 180, 213, 224 and 211F, respectively. The LTO700 exhibits high capacitance superior to

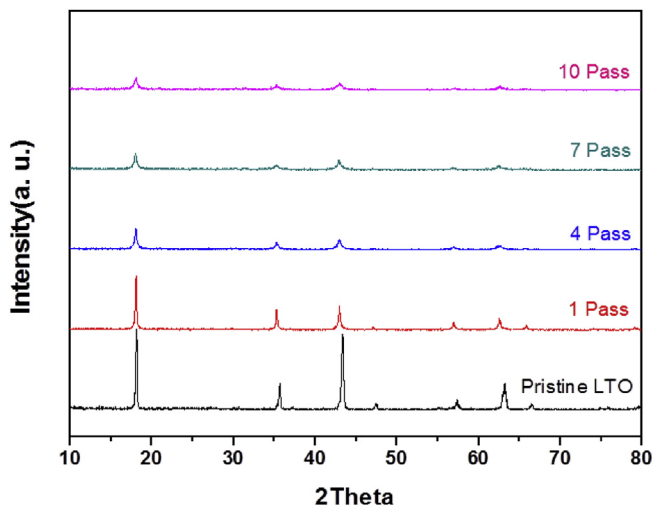


Fig. 3. X-ray diffraction patterns of pristine $\text{Li}_4\text{Ti}_5\text{O}_{12}$ and $\text{Li}_4\text{Ti}_5\text{O}_{12}$ powders prepared by high-energy milling 1, 4, 7, and 10 times pass.

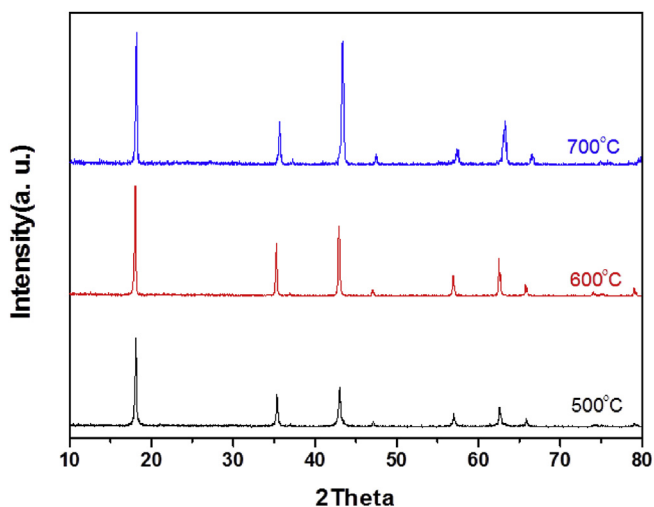


Fig. 4. X-ray diffraction patterns of the $\text{Li}_4\text{Ti}_5\text{O}_{12}$ powders treated by post-calcination at various temperatures from 500 to 700 °C.

pristine $\text{Li}_4\text{Ti}_5\text{O}_{12}$. Therefore, correlation between improved crystallinity and small particle size is expected.

Fig. 7 shows the rate capabilities of pristine $\text{Li}_4\text{Ti}_5\text{O}_{12}$ and $\text{Li}_4\text{Ti}_5\text{O}_{12}$ treated by post-calcination at different discharge rates from 1 to 20 A. The capacity retention was examined by discharge capacity at 20 A in comparison with that at 1 A. The pristine LTO,

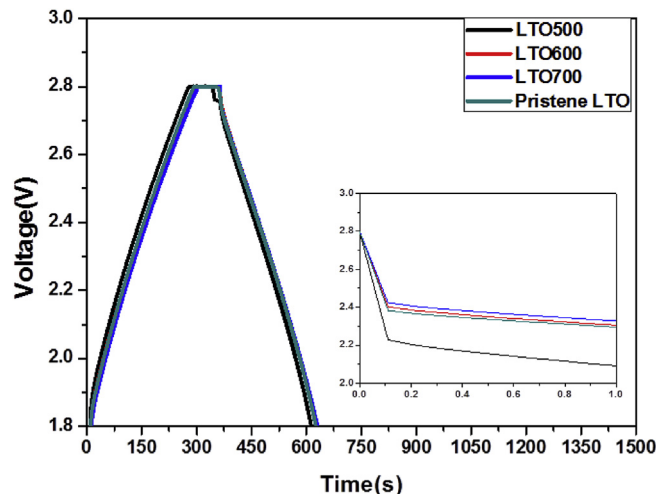


Fig. 6. Charge and discharge curves of the hybrid capacitors using the LTO500, LTO600, LTO 700, and pristine LTO at 1 A.

LTO 500, and LTO600 show capacity retention of 65.0, 50.5, 70.9%, respectively. It was confirmed that each capacity retention corresponds to the initial IR-drop depicted in Fig. 6. The LTO700 shows remarkably improved rate capability, especially at 20 A, that it performs with capacity retention above 75%. It can be seen that the rate capability was inversely proportional to the internal resistance. The electrochemical properties of hybrid capacitors depend heavily on the crystallinity of $\text{Li}_4\text{Ti}_5\text{O}_{12}$. Improved crystallinity and small particle size by post-calcination and high energy milling cause excellent rate capabilities.

Electrochemical impedance spectroscopy may be considered as one of the most sensitive tools for the study of differences in electrode behavior. The electrochemical impedance spectra for the hybrid capacitors, as presented in Fig. 8, shows the AC impedance spectra of the LTO500, LTO600, LTO700 and pristine LTO. In the equivalent circuit, the semicircle related to transfer of charge and lithium ion at the electrode/electrolyte interface could be observed at high frequency in all cells. The charge transfer resistance (R_{ct}) was indicated on the Z-axis, which means ohmic resistance. The straight lines in the low frequency range represent the Warburg impedance of long-range Li-ion diffusion through the $\text{Li}_4\text{Ti}_5\text{O}_{12}$ electrode [18]. It can be obviously seen that the resistance of nano-sized $\text{Li}_4\text{Ti}_5\text{O}_{12}$ prepared by post calcination is lower than the pristine one. Hence, it demonstrates that good particle distribution and small particle size can significantly improve the electrochemical kinetics of $\text{Li}_4\text{Ti}_5\text{O}_{12}$ and decrease their resistance. However, for the LTO500, the resistance of the hybrid capacitor is higher than the pristine LTO. These results suggest that the resistance increases with the decrease the crystallinity of $\text{Li}_4\text{Ti}_5\text{O}_{12}$.

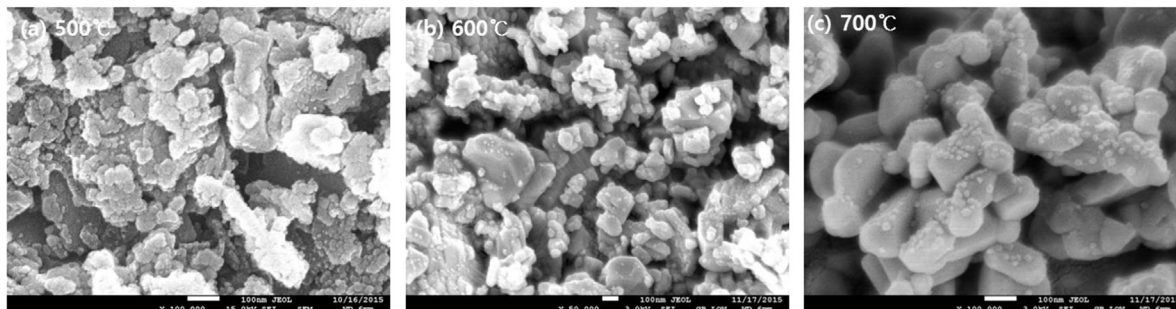


Fig. 5. SEM images of $\text{Li}_4\text{Ti}_5\text{O}_{12}$ powders treated by post-calcinations at (a) 500 °C, (b) 600 °C, and (c) 700 °C.

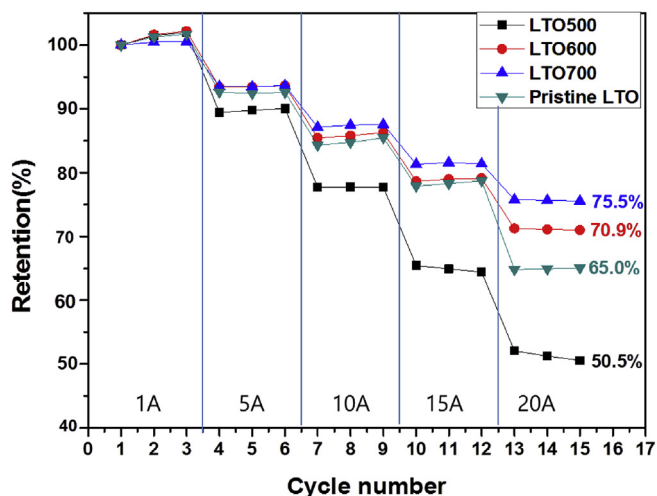


Fig. 7. Different discharge rates of hybrid capacitors using $\text{Li}_4\text{Ti}_5\text{O}_{12}$ treated by post-calcination at 500, 600, and 700 °C. The cells were charged and discharged at various current rates varying from 1 to 20 A.

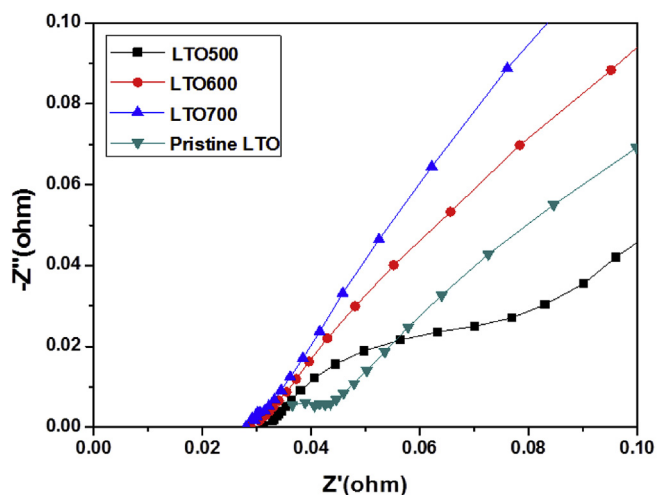


Fig. 8. Electrochemical impedance spectra curves of the hybrid capacitors using $\text{Li}_4\text{Ti}_5\text{O}_{12}$ treated by post-calcination at 500, 600, and 700 °C negative electrode at the voltage of 2.8 V.

Fig. 9 shows the cycling performance of hybrid capacitors with the LTO500, LTO600, LTO700 and pristine LTO negative electrode at the high current density of 5 A. The initial reversible specific capacity of LTO500, LTO600, LTO700 and pristine $\text{Li}_4\text{Ti}_5\text{O}_{12}$ cell is 64.4, 77.3, 80.3 and 76.7 mAh, respectively. The LTO700 exhibits cycling performance superior to pristine $\text{Li}_4\text{Ti}_5\text{O}_{12}$. Among all cells, LTO700 has the highest discharge capacity and capacity retention of 99.9% after 1500 cycles. This suggests that nano-sized $\text{Li}_4\text{Ti}_5\text{O}_{12}$ with good crystallinity can shorten Li-ion diffusion pathway, favoring Li-ion mobility and enhancing cyclability and high rate performance.

4. Conclusion

We developed a new preparation route for $\text{Li}_4\text{Ti}_5\text{O}_{12}$ with nano particles using high-energy milling and studied its properties in hybrid capacitors. Our synthesis approaches using high-energy milling and post-calcination allowed the formation of 100 nm grade $\text{Li}_4\text{Ti}_5\text{O}_{12}$ featuring a higher crystallinity than the pristine one

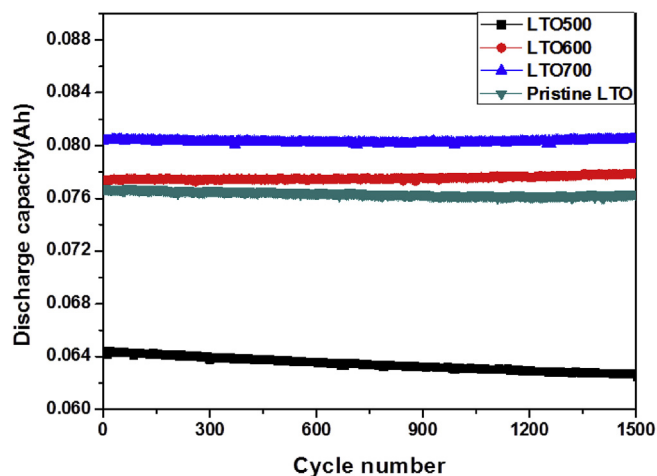


Fig. 9. Cycling performance of the hybrid capacitors using $\text{Li}_4\text{Ti}_5\text{O}_{12}$ treated by post-calcination at 500, 600, and 700 °C negative electrode at 5 A.

prepared by a conventional solid-state reaction at 900 °C. The LTO700 showed much better rate capability than pristine $\text{Li}_4\text{Ti}_5\text{O}_{12}$. Even at 20 A, LTO700 also keeps 75.5% of capacity compared with 1 A. The cyclability of $\text{Li}_4\text{Ti}_5\text{O}_{12}$ exhibits capacity retention of 99.9% after 1500 cycles. The excellent rate capability and cycling performance are mainly attributed to the small particle size and high crystallinity of $\text{Li}_4\text{Ti}_5\text{O}_{12}$ prepared by high energy milling and post-calcination. Hence, the hybrid capacitor using LTO700 negative electrode can be regarded as a potential energy storage device for high power applications.

Acknowledgments

This study was supported by the Energy Efficiency & Resources of the Korea Institute of Energy Technology Evaluation and Planning (KETEP) grant funded by the Korea government Ministry of Knowledge Economy (20142020103060). It was also supported by the Industrial Fundamental Technology Development Program (10052745) funded by the Ministry of Trade, Industry and Energy (MOTIE) of Korea.

References

- [1] T. Yuan, R. Cai, K. Wang, R. Ran, S. Liu, Z. Shao, *Ceram. Int.* 35 (2009) 1757.
- [2] A. Sivashanmugam, S. Gopukumar, R. Thirunakaran, C. Nithya, S. Prema, *Mater. Res. Bull.* 46 (2011) 492.
- [3] Z. Huang, D. Wang, Y. Lin, X. Wu, P. Yan, C. Zhang, D. He, *J. Power Sources* 266 (2014) 60.
- [4] A. Riduan, M. Faisal, G.S. Chung, *Trans. Elect. Electron. Mater.* 13 (2012) 125.
- [5] M.M. Thackeray, *J. Electrochem. Soc.* 142 (1995) 2558.
- [6] S. Scharner, W. Weppner, P. Schmind-Beurmann, *J. Electrochem. Soc.* 146 (1999) 857.
- [7] K. Zaghib, M. Armand, M. Gauthier, *J. Electrochem. Soc.* 145 (1998) 3135.
- [8] Y.H. Rho, K. Kanamura, *J. Solid State Chem.* 177 (2004) 2094.
- [9] C.Y. Ouyang, Z.Y. Zhong, M.S. Lei, *Electrochem. Commun.* 9 (2007) 1107.
- [10] K. Zaghib, M. Simoneau, M. Armand, M. Gauthier, *J. Power Sources* 81 (1999) 300.
- [11] G.G. Amatucci, F. Badway, A. Du Pasquier, T. Zheng, *J. Electrochem. Soc.* 148 (2001) 930.
- [12] K. Kanamura, N. Akutagawa, K. Dokko, *J. Power Sources* 146 (2005) 86.
- [13] D. Pasquiera, C.C. Huang, T. Spitzer, *J. Power Sources* 186 (2009) 508.
- [14] B.G. Lee, J.R. Yoon, *Curr. Appl. Phys.* 13 (2013) 1350.
- [15] D.L. Zhang, *Prog. Mater. Sci.* 49 (2004) 537.
- [16] Q. Wang, Z. Wen, J. Li, *Adv. Funct. Mater.* 16 (2006) 2141.
- [17] J.Y. Luo, Y.Y. Xia, *J. Power Sources* 186 (2009) 224.
- [18] J.J. Huang, Z.Y. Jiang, *J. Electrochim. Acta* 53 (2008) 7756.



Site Search

Customer Care Training

Clarivate > Master Journal List > Journal Search

JOURNAL SEARCH

**SUBMITTING
A JOURNAL?**

Build bibliographies
in more than 5,000
different styles.

with **EndNote**[®]
endnote.com >

Search Terms: 1567-1739

Total journals found: 1

THE FOLLOWING TITLE(S) MATCHED YOUR REQUEST:

Journals 1-1 (of 1)

<< < > >>

[FORMAT FOR PRINT](#)

CURRENT APPLIED PHYSICS

Bimonthly ISSN: 1567-1739

ELSEVIER SCIENCE BV, PO BOX 211, AMSTERDAM, NETHERLANDS, 1000 AE

Coverage

[Science Citation Index](#)

[Science Citation Index Expanded](#)

[Current Contents - Physical, Chemical & Earth Sciences](#)

Journals 1-1 (of 1)

<< < > >>

[FORMAT FOR PRINT](#)

Search Terms:

Search type:

Database:

[SEARCH](#)